Chemical Science

ROYAL SOCIETY OF CHEMISTRY

EDGE ARTICLE

View Article Online
View Journal | View Issue

Cite this: *Chem. Sci.*, 2024, **15**, 11794

All publication charges for this article have been paid for by the Royal Society of Chemistry

Repurposing a supramolecular iridium catalyst *via* secondary Zn···O=C weak interactions between the ligand and substrate leads to *ortho*-selective C(sp^2)–H borylation of benzamides with unusual kinetics†

Jonathan Trouvé,[a] Vanessa Delahaye,[a] Michele Tomasini,[b] Purushothaman Rajeshwaran,[a] Thierry Roisnel,[a] Albert Poater *[b] and Rafael Gramage-Doria *[a]

The iridium-catalyzed C–H borylation of benzamides typically leads to *meta* and *para* selectivities using state-of-the-art iridium-based *N*,*N*-chelating bipyridine ligands. However, reaching *ortho* selectivity patterns requires extensive trial-and-error screening *via* molecular design at the ligand first coordination sphere. Herein, we demonstrate that triazolylpyridines are excellent ligands for the selective iridium-catalyzed *ortho* C–H borylation of tertiary benzamides and, importantly, we demonstrate the almost negligible effect of the first coordination sphere in the selectivity, which is so far unprecedented in iridium C–H bond borylations. Remarkably, the activity is dramatically enhanced by exploiting a remote Zn···O=C weak interaction between the substrate and a rationally designed molecular-recognition site in the catalyst. Kinetic studies and DFT calculations indicate that the iridium-catalyzed C–H activation step is not rate-determining, this being unique for remotely controlled C–H functionalizations. Consequently, a previously established supramolecular iridium catalyst designed for *meta*-borylation of pyridines is now compatible with the *ortho*-borylation of benzamides, a regioselectivity switch that is counter-intuitive regarding precedents in the literature. In addition, we highlight the role of the cyclohexene additive in avoiding the formation of undesired side-products as well as accelerating the HBpin release event that precedes the catalyst regeneration step, which is highly relevant for the design of powerful and selective iridium borylating catalysts.

Received 5th March 2024
Accepted 10th June 2024

DOI: 10.1039/d4sc01515k

rsc.li/chemical-science

Introduction

The functionalization of C–H bonds by means of transition metal catalysis is one of the most powerful methodologies in chemical synthesis as it provides access to highly elaborated molecules with step- and atom-economy in a predictive manner.[1] Consequently, compounds difficult or impossible to form otherwise are nowadays accessible,[2] which is relevant for drug discovery in the application of late-stage functionalization methodologies for upgrading the available chemical space[3] as well as in the area of materials sciences to find chemical systems featuring unique photo-, electro- and physicochemical properties.[4] Traditionally, the directing group present in the substrate of interest directs the selectivity *via* metal-coordination in C–H bond functionalizations.[5] Consequently, it is highly important to develop selective metal-catalysed C–H bond functionalizations for unbiased substrates, thus reducing the costs devoted to the introduction and further removal of metal-coordinating directing groups.[6]

In this context, C–B bond-forming processes *via* C–H activation employing iridium catalysts are particularly attractive since they take place without the need of covalently linking directing groups to the substrate of interest[7] and well-known methodologies can be applied to further transform the boron-based functional group into more useful carbon- or heteroatom-containing fragments.[8] Indeed, the reactivity and the selectivity at iridium are highly affected by the nature of the ligand attached to it, with neutral bipyridine-type ligands being of choice since the pioneering contributions by Ishiyama, Miyaura and Hartwig.[9]

[a]*Univ Rennes, CNRS, ISCR – UMR 6226, F-35000 Rennes, France. E-mail: rafael.gramage-doria@univ-rennes1.fr*

[b]*Departament de Química, Institut de Química Computacional i Catàlisi, Universitat de Girona, c/Maria Aurèlia Capmany 69, 17003 Girona, Catalonia, Spain. E-mail: albert.poater@udg.edu*

† Electronic supplementary information (ESI) available. CCDC 2216009. For ESI and crystallographic data in CIF or other electronic format see DOI: https://doi.org/10.1039/d4sc01515k

In the case of aromatic substrates the iridium-catalysed C–H bond borylation generally occurs at the less sterically demanding *meta* and *para* positions.[10] This regio-selectivity is largely controlled by the rational design of catalysts enabling attractive substrate-to-ligand interactions *via* hydrogen bonding or ion-pairing in view to place a specific C–H bond at close spatial proximity of the active *N*,*N*-chelated iridium site.[11] In the case of benzamides, which are important constituents in agrochemicals[12] and active pharmaceutical ingredients,[13] the selective iridium-catalysed C–H bond borylation at *meta* and *para* positions, respectively, were accomplished with unique iridium catalysts developed, independently, by Kuninobu and Kanai, Phipps, Chattopadhyay, and Nakao.[14] In the case of iridium-catalysed *ortho* C–H bond borylations (Fig. 1A), Reek developed a neutral bipyridine ligand featuring a hydrogen bonding site that works specifically for secondary benzamides (Fig. 1B).[15] On the other hand, *ortho* C–H bond borylations of tertiary benzamides were disclosed utilizing anionic hybrid chelating ligands as shown by Maleczka and Smith (P,Si- or N,Si-chelating ligands) and by Chattopadhyay (N,$C_{thienyl}$- or N,C_{furyl}-chelating ligands) (Fig. 1B).[16a–c] A series of ligands enabling iridium-catalysed *ortho* C–H bond borylations of tertiary benzamides with modest activity were reported by Li and co-workers.[16d,e]

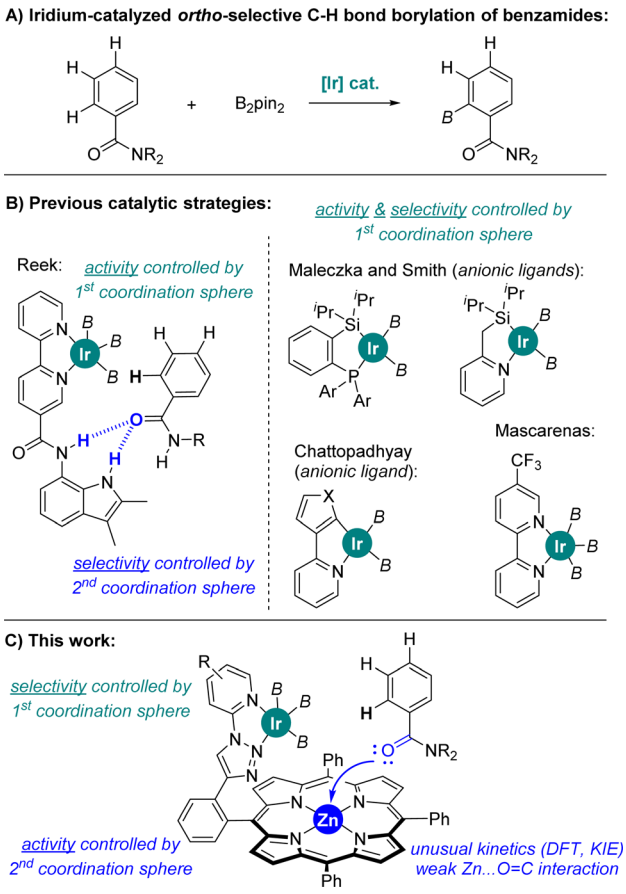

Fig. 1 Previous catalysts enabling *ortho*-selective C–H bond borylation of benzamides (A and B) and the current, repurposed supramolecular approach (C). B_2pin_2 = bis(pinacolato)diboron, *B* = (pinacolato)boron, Ar = *para*-tolyl, X = O, S.

Recently, Mascareñas and co-workers reported a neutral CF_3-containing bipyridine ligand that led to iridium-catalysed *ortho* C–H borylated benzamides after extensive trial-and-error ligand screening (Fig. 1B).[16f] Sawamura also reported *ortho* C–H borylation of a single example of tertiary benzamide with a heterogeneous phosphine–iridium system supported on silica.[16g] Iridium-catalysed *ortho* C–H bond borylations of phenol, aniline and thioanisole derivatives have been achieved exploiting remote weak interactions between the boryl ligands and the functional group in the arene, as well as between Lewis acid boron-containing motifs in the bipyridine ligand and the Lewis base thioether group in the substrate.[16h–j] In all the above-stated examples, the rather air-sensitive $[Ir(COD)(OMe)]_2$ was used as the catalyst precursor,[14–16] and the iridium-catalysed C–H bond activation step was found to be the rate-determining step of the catalytic cycle for the cases in which this was studied.[9–16] Note that palladium- and iron-catalysed *ortho*-selective C–H bond borylations are known.[16k,l]

Ultimately, predicting the reactivity of an iridium C–H bond borylating catalyst in a precise manner is a major goal. Herein, we report a predictive catalyst design based on a supramolecular strategy that enables the highly *ortho* selective C–H bond borylation of tertiary benzamides employing a neutral triazolylpyridine-chelating ligand and a rather air stable $[Ir(COD)(Cl)]_2$ metal precursor. The iridium catalyst is built up around a zinc-porphyrin unit that enables a unique Zn···O=C weak interaction between the amide group in the substrate and the catalyst in a remote fashion (Fig. 1C). Extensive control experimentation and catalyst evaluation demonstrate that the selectivity is exclusively controlled by the iridium-ligated triazolylpyridine-*N*,*N*-chelating site regardless of its chemical nature at the first coordination sphere, whereas the activity is highly enhanced thanks to the crucial substrate preorganization occurring at the second coordination sphere *via* a single, remote Zn···O=C weak interaction. In addition, computational calculations predicted that the iridium-mediated C–H bond activation is not the rate-determining step, but rather the iridium-mediated C–B bond formation, analogous to Chirik's pincer-type cobalt-catalysed borylations.[17] This unexpected feature, which explains the observed reactivity of the supramolecular iridium catalyst, was further supported by kinetic isotopic effect studies.

Results and discussion

Considerations for catalyst rationale

Previously, we reported on the *meta* selective C(sp^2)–H bond borylation of pyridines using a well-defined supramolecular iridium catalyst equipped with a zinc-porphyrin unit that served for the specific molecular recognition of pyridines *via* a remote Zn···N weak coordination bond (Fig. 2, top, left).[18] In order to demonstrate the generality of this approach, we reasoned that other molecules different than nitrogen-containing heterocycles such as benzamides could potentially bind in a reversible manner to the zinc centre of the molecular recognition site, thereby placing potentially reactive C–H sites at close proximity of the catalytically active iridium site. During the course of our

studies, we successfully obtained single crystals suitable for X-ray diffraction studies upon slow evaporation of a dichloromethane solution containing a zinc(II)-tetraphenylporphyrin (ZnTPP) and *N*,*N*-dimethylformamide (DMF).[19] Analogously to the well-known binding of other tertiary amides to zinc-porphyrin derivatives,[20] the DMF molecule apically binds to the zinc centre of ZnTPP *via* the oxygen atom (Fig. 2, top, right). With these considerations, we built a PM3 semi-empirical molecular model combining our supramolecular iridium catalyst with *N*,*N*-dimethylbenzamide as the substrate because it could match for C(sp^2)–H borylation similar to that for pyridines (Fig. 2). Interestingly, this low-cost prediction suggests that the supramolecular iridium catalyst might be suitable for activating the aromatic *ortho* C–H bond of the benzamide instead of the anticipated *meta* one. In fact, the *ortho* C–H bond of the benzamide is located at a distance of four chemical bonds apart from the molecular recognition site, a distance that is exactly the same for the case of pyridine substrates. As such, a single, remote Zn···X (X = N or O=C) weak interaction between the substrate and the catalyst could be enough to reverse the regioselectivity between pyridines and benzamides. The fact that the distance and geometry between the active site and the substrate recognition site in this supramolecular approach are key parameters results in a slight influence of the substrate electronic effects on controlling the catalytic outcome. On the other hand, such strategy takes advantage of the difference in the coordinating ability between a cationic iridium that will have more affinity for anionic boryl ligands and a neutral amide that will have more affinity to a neutral zinc-porphyrin unit in agreement with the hard and soft acid and base theory.[21] Consequently, this supramolecular approach would lead to an iridium catalyst that will switch the selectivity (from *meta* to *ortho*) between pyridines and benzamides, which strikingly contrasts with the pioneering Nakao's observations in which the same iridium, boron-based catalyst led to the same *meta* regioselectivity for both pyridines and benzamides (Fig. 2, bottom).[14f] Note that Nakao's group reported Ir/Al-based catalysts that afforded *para*-borylated products for both pyridines and benzamides.[14a]

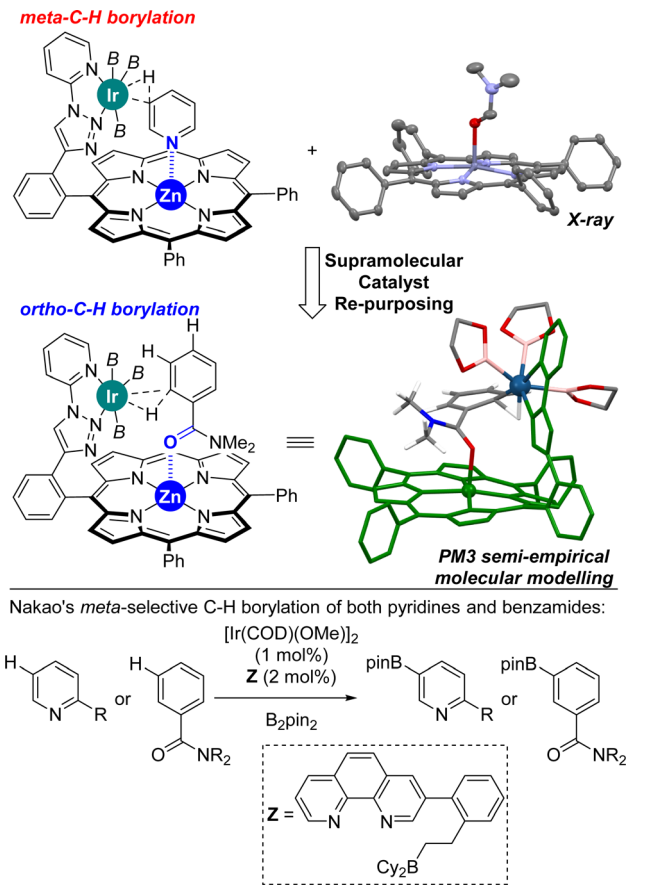

Fig. 2 Previous supramolecular iridium-catalysed *meta*-C–H bond borylation of pyridines (top, left), ORTEP of [ZnTPP ⊂ DMF] determined by single-crystal X-ray diffraction studies (thermal ellipsoids at 50% probability, all hydrogen atoms are omitted, top, right), and current re-purposed supramolecular iridium-catalysed *ortho*-C–H borylation of benzamides with the PM3-minimized molecular modelling for a plausible intermediate (the methyl groups on the boryl ligand and all hydrogen atoms except those of the amide in the substrate were omitted). Previous iridium-catalysed C–H borylation of both pyridines and benzamides with the same ligand and the same *meta*-selectivity (bottom). B_2pin_2 = bis(pinacolato)diboron, *B* = (pinacolato)boron.

Validation of the supramolecular catalyst action mode: ligand assessment, control experimentation, computational calculations and kinetic studies

Taking the above-stated rationale into consideration, we evaluated the supramolecular ligands **L1–L6**, which comprise different steric and electronic substituents at the triazolylpyridine site while keeping the same molecular recognition site made of a zinc-porphyrin backbone, in the iridium-catalysed C–H bond borylation of *N*,*N*-dimethylbenzamide (**1a**) as the model substrate (Fig. 3 and Table S1 in the ESI†). For comparison purposes, we also assessed the corresponding triazolylpyridine ligands lacking the zinc-porphyrin substrate recognition site (**L1*–L6***, Fig. 3). For the sake of comparison with our previously developed *meta*-selective C–H borylation of pyridines,[18] the reactions were evaluated at 80 °C using *para*-xylene as the solvent and 1.5 equivalents of the borylating reagent B_2pin_2 (Fig. 3).

In terms of conversion of **1a**, the iridium-catalysed C–H bond borylation employing each supramolecular ligand **L** outperformed its non-supramolecular counterpart **L*** by at least a factor of two (blue bars and dashed lines, Fig. 3). On the other hand, the *ortho*-selectivity was comparable for all supramolecular catalysts derived from **L1–L6** being in the range of 89–97% (green colour, Fig. 3). Although this selectivity compares well with previous precedents,[16] the major difference of our supramolecular approach is that there is a negligible effect of the first coordination sphere regarding the selectivity outcome of the catalysis. In contrast, and as was expected, using the classical 4,4′-di-*tert*-butyl-2,2′-bipyridine (dtbpy) ligand afforded a mixture of *meta* and *para* borylated products (red colour, Fig. 3) with a complete absence of formation of the *ortho* isomer. These findings clearly indicate that the selectivity of this

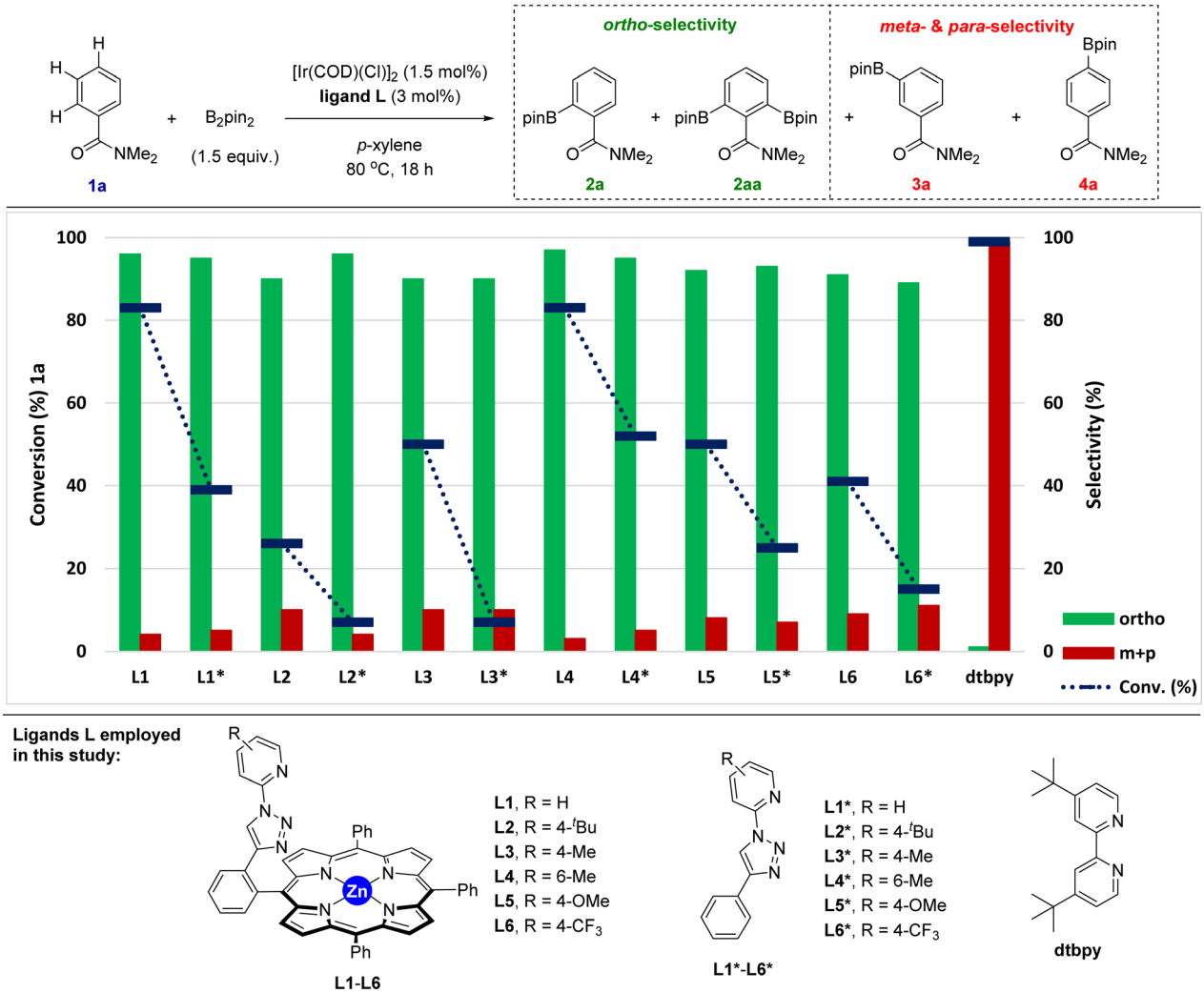

Fig. 3 Assessment of the supramolecular and non-supramolecular ligands in the iridium-catalysed C–H bond borylation of *N*,*N*-dimethylbenzamide **1a**. Reaction conditions: **1a** (0.024 g, 0.162 mmol), $[Ir(COD)(Cl)]_2$ (1.7 mg, 2.43×10^{-3} mmol), ligand **L** (4.86×10^{-3} mmol), B_2pin_2 (61.7 mg, 0.243 mmol), *p*-xylene (1 mL), 80 °C, 24 h (conversion of **1** and product selectivity for **2**/**3**/**4** were determined by GC analysis using dodecane as internal standard and ^1H NMR analysis).

transformation when using the supramolecular ligands **L1–L6** is exclusively controlled by the trivial iridium-coordinated triazolylpyridine unit in the first coordination sphere and that the activity is enhanced by the presence of the substrate recognition zinc-porphyrin site in the second coordination sphere.

The best results in terms of selectivity (97% *ortho*-selectivity) and activity (83% conversion) were encountered for the supramolecular ligands **L1** and **L4** (Fig. 3), most notably, without the need to employ an $[Ir(COD)(OMe)]_2$ metal precursor, which is in stark contrast with precedents in the literature.[7–16] At this stage, the exact action mode of the non-supramolecular catalysts derived from ligands **L1*–L6*** remains to be addressed without discarding the potential role of the amide unit within the substrate as an *ortho*-directing group.[22] However, for the case of the supramolecular catalysts derived from **L1–L6**, CPK models indicate that the large porphyrin backbone comprising three bulky phenyl groups in the ligand strongly disfavour the accommodation of the benzamide substrate by *ortho*-chelation around the catalytically productive iridium-$(boryl)_n$ species (n = 2 or 3) due to steric shielding. In other words, the highly sterically congested supramolecular iridium catalysts derived from ligands **L1–L6** give no choice to the benzamide substrate than engaging in a Zn···O=C weak interaction upon approaching the catalyst. In addition, similar to our previous observations using pyridines as substrates in metal catalysis,[18,23] such a supramolecular effect was completely lost in the presence of polar coordinating solvents such as THF, DMF or 1,4-dioxane, which disrupt the remote Zn···O=C weak interaction by solvent-coordination to the zinc centre of the porphyrin backbone *via* Zn···O interaction. Aside from the key substrate-preorganization effects, increasing the effective molarity of the substrate around the catalyst is also a major advantage of the supramolecular iridium catalysts derived from **L1–L6.**

The only difference between the supramolecular iridium catalysts derived from **L1** and **L4** was the ratio of mono- *versus* bis-borylation, *i.e.* **2a** : **2aa** (Scheme 1). Using **L1** afforded an 81 :

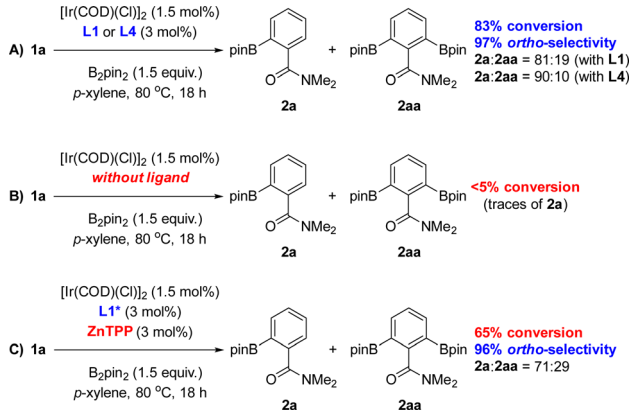

Scheme 1 Reaction conditions applied with the optimal supramolecular ligands **L1** and **L4** (A) and control experimentation (B and C). ZnTPP = zinc(II)-tetraphenylporphyrin.

19 ratio of **2a : 2aa** (Scheme 1A), whereas the bulkier **L4** containing a 6-methyl-substitution pattern in the iridium-coordinated pyridine moiety led to an increased mono-selectivity of **2a : 2aa** = 90 : 10 ratio (Scheme 1A). This finding was explained by the significant steric shielding that needs to be overcome in order to get a second borylation in compound **2a** within the supramolecular iridium catalyst derived from **L4**. Additional experiments demonstrate the lack of reactivity when the catalytic reactions were carried out in the absence of any ligand (Scheme 1B). To further understand the unique behaviour of the supramolecular ligand **L1** in the *ortho*-selective C–H bond borylation of benzamide **1a**, a reaction was carried out using the molecular-recognition-free ligand **L1*** and **ZnTPP** at 3 mol% loading each (Scheme 1C). Whereas 96% *ortho*-selectivity was obtained, showing again the importance of the metal-coordinated triazolylpyridine ligand backbone, the conversion of **1a** significantly dropped to 65% (Scheme 1C) when compared to the supramolecular version **L1** (83% conversion of **1a**, Scheme 1A). These control experiments demonstrate the requirement of covalently linking the triazolylpyridine fragment to the substrate recognition site to increase the reactivity of the catalyst.

Interestingly, the amount of bis-functionalized borylated product significantly increased (**2a : 2aa** = 71 : 29, Scheme 1C) when compared to the reaction carried out in the presence of the supramolecular ligand **L1** (**2a : 2aa** = 81 : 19, Scheme 1A). This observation suggests that the supramolecular ligands are rather bulky and disfavour to some extent the second borylation pathway towards **2aa**. Although the binding of amide groups to zinc-porphyrin derivatives is well known including our X-ray data (Fig. 2),[20] we did not succeed in detecting direct evidence of the Zn···O=C weak interaction between the supramolecular ligand **L1** and the benzamide substrate **1a** in solution by titration NMR studies (^{1}H, ^{13}C and DOSY) because this is known to be a very fast exchange process at the NMR time scale.[24] In fact, solvents such as amides (*i.e.* DMF) and other oxygen-containing derivatives (*i.e.* acetone, THF, DMSO) are typically used to cleave porphyrin aggregates leading to mono-nuclear and discrete, solvated-zinc-porphyrin species involving Zn···O interaction.[24] On the other hand, attempts to carry out UV-vis titration studies between the ligand **L1** and the benzamide substrate **1a** did not provide accurate data for determining the eventual association constant. This is hardly surprising as the association constant between amides and zinc-porphyrins is known to be significantly lower than 10^2 M^{-1}.[20d] Nevertheless, the real situation during the catalysis might be different compared to the specific binding between the ligand **L1** and the substrate **1a** as the iridium site will provide further affinity towards the substrate for activating a C–H bond while simultaneous Zn···O=C weak interaction occurs at the molecular recognition site. In other words, the supramolecular catalyst may have a stronger affinity for the transition state rather than for the substrate as was observed before for the *meta*-selective C–H borylation of pyridines[18] and previously by Sanders using zinc-porphyrins as organocatalysts.[25]

The sensitivity to steric shielding associated with the supramolecular iridium catalyst derived from ligand **L1** was additionally addressed by evaluating the reactivity of the benzamides **1a–1e** bearing different substituents around the nitrogen atom (Fig. 4). For comparison purposes, reaction time of the C–H borylation was kept at 24 hours to ensure the maximum reactivity for each substrate at 80 °C (instead of 18 hours in Fig. 3 and Scheme 1). The supramolecular iridium catalysis was highly affected under these reaction conditions by the steric nature of the tertiary amide group with the conversion

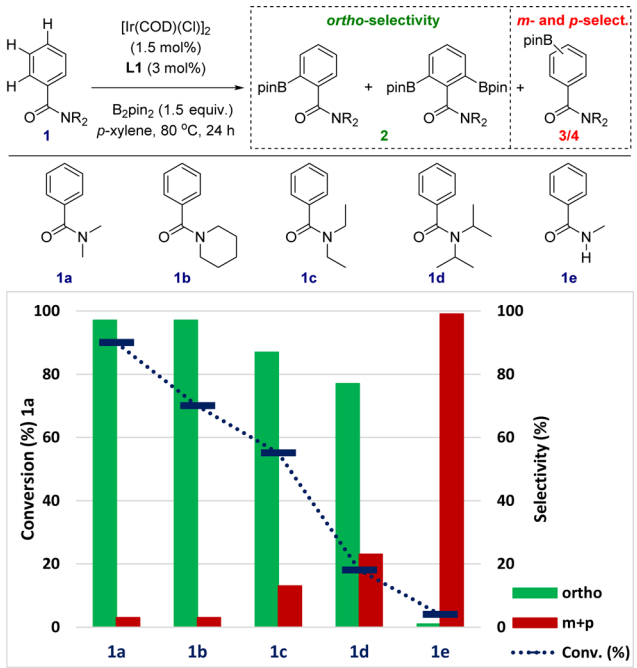

Fig. 4 Relevance of the steric parameters of the amide group in benzamides **1a–1e** for the supramolecular iridium-catalysed C–H borylation. Reaction conditions: **1** (0.162 mmol), [Ir(COD)(Cl)]$_2$ (1.7 mg, 2.43×10^{-3} mmol), **L1** (4.1 mg, 4.86×10^{-3} mmol), B_2pin_2 (61.7 mg, 0.243 mmol), *p*-xylene (1 mL), 80 °C, 24 h (conversion of **1** and product selectivity for **2/3/4** were determined by GC analysis using dodecane as internal standard and ^{1}H NMR analysis).

decreasing from 90% for **1a** to 18% for the bulkiest iso-propyl substituent in **1d** (blue colour, Fig. 4). Importantly, the *ortho*-selectivity was still remarkable ranging from 97% in the best case (**1a** and **1b**) to 87% for **1c** and 77% for the challenging **1d** (green colour, Fig. 4). The formation of both *meta*- and *para*-borylated side-products **3** and **4** increased to 13% for **1c** and 23% for **1d**, respectively (red colour, Fig. 4), in line with an increase of the steric shielding associated with these substrates that may disfavour the remote Zn···O=C weak interaction between the substrate and the supramolecular catalyst. In the case that the reaction would be controlled by the classical amide-directed iridium-chelation, little difference of reactivity should have been found, which is not the case for the current case of study with the supramolecular ligand **L1**.

Secondary benzamides such as **1e** were not compatible with this supramolecular iridium catalysis (Fig. 4). The almost absence of reactivity encountered in **1e** was attributed to (i) the poorer coordinating ability of the carbonyl group due to tautomerization[22] and/or (ii) catalyst inhibition due to *N*-coordination to iridium with HBpin release.[26] Overall, the above-stated observations strongly suggest the postulated action mode in which the remote Zn···O=C weak interaction is beneficial for increasing the reactivity of the catalysis.

In view to further rationalize such findings, Densitiy Functional Theory (DFT) calculations were performed to unravel the mechanism associated with the *ortho*-C–H borylation of benzamide **1a** using the supramolecular ligand **L1** at 80 °C. The DFT-computed reaction mechanism is shown in Scheme 2 and the following conclusions can be drawn:

(1) The substrate bound to the catalyst (complex **A**) *via* remote Zn···O=C interaction is less favoured with benzamides ($\Delta G^{\circ}_{353K} = +5.6$ kcal mol^{-1}) than with pyridines *via* Zn···N interaction ($\Delta G^{\circ}_{353K} = +1.4$ kcal mol^{-1}),[18b] thereby supporting the previous findings (*vide supra*) that indicated the relatively low affinity of benzamides to the zinc-porphyrin molecular recognition pocket compared to pyridines, but still being energetically accessible.

(2) The *ortho*-C–H activation step (**A** → **B**) requires an energetic barrier of $\Delta G^{\ddagger} = +31.7$ kcal mol^{-1}, which is slightly lower than that observed for the *meta*-C–H activation of pyridine that was found to be $\Delta G^{\ddagger} = +33.7$ kcal mol^{-1}.[18] Consequently, the iridium-mediated C–H activation and remote Zn···O=C interaction between the ligand and the substrate contribute simultaneously in a cooperative manner to decreasing the energetic barrier of this key transition state in the benzamide case. Note that DFT calculations considering the cleavage of the Zn···O=C

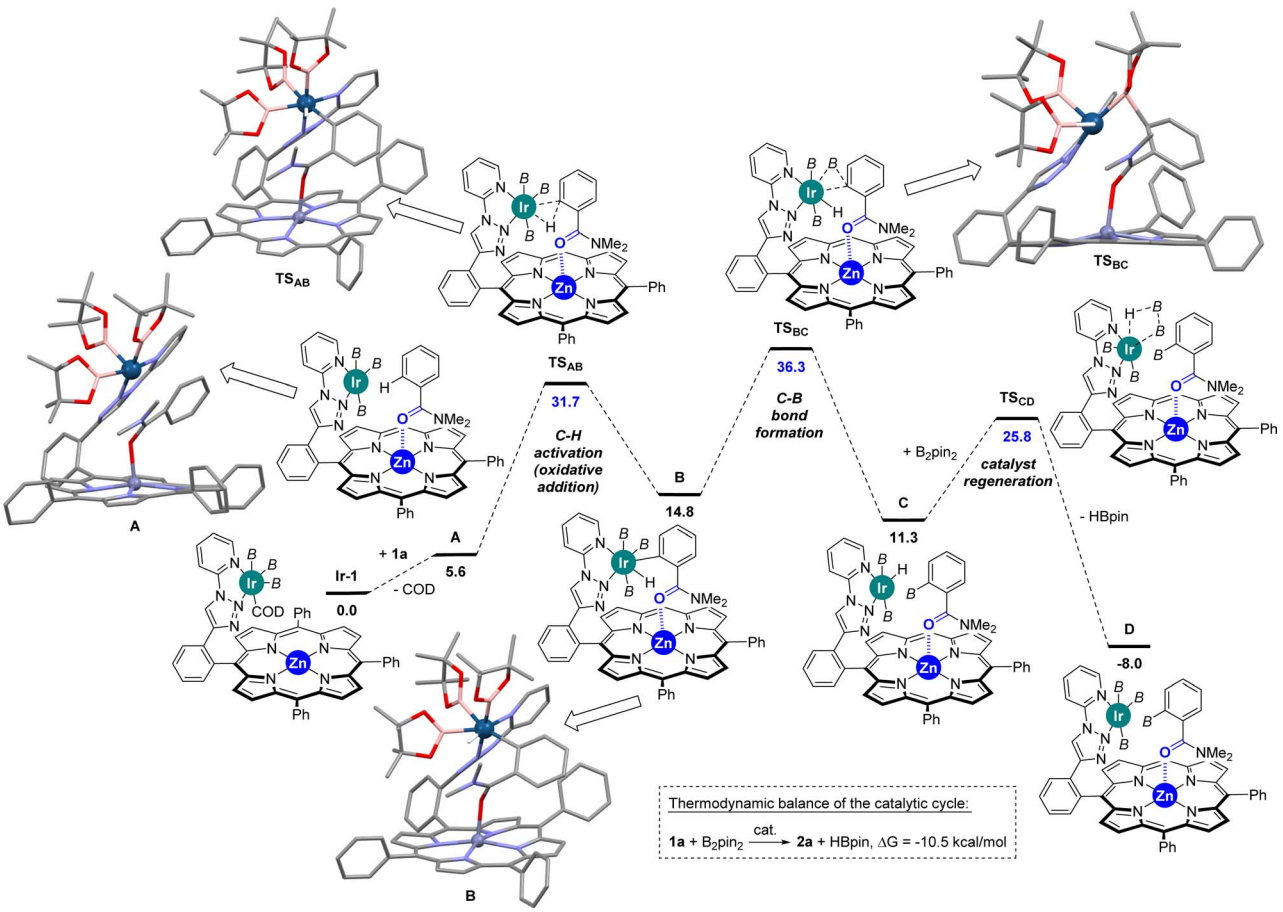

Scheme 2 DFT-computed energetic profile of the reaction mechanism for the supramolecular iridium-catalysed *ortho*-C–H borylation of the benzamide **1a** using the supramolecular ligand **L1** (Gibbs energies at 353 K in kcal mol^{-1}; in blue the relative energies corresponding to the transition states). *B* = (pinacolato)boron.

interaction did not afford any other stable intermediate and that the Zn···O=C interaction was restored (κ^2-N,O-coordination of the substrate to the zinc centre was also ruled out by DFT calculations).

(3) The C–B bond-forming step (**B** → **C**), which is $\Delta G^{\ddagger}$ = +36.3 kcal mol^{-1}, is unexpectedly higher in energy compared to the C–H activation step (**A** → **B**). Consequently, the C–B bond-forming step appears to be the rate-determining one in the supramolecular iridium-catalysed *ortho*-C–H borylation of benzamide. For comparison purposes, it is relevant to note that the C–B bond-forming step (**B** → **C**) for the *meta*-C–H borylation of pyridine was computed to be $\Delta G^{\ddagger}$ = +27.1 kcal mol^{-1},[18] a value which is significantly lower than that observed for benzamides.

(4) Catalyst regeneration is accessible with a relatively low barrier of $\Delta G^{\ddagger}$ = +25.8 kcal mol^{-1} and the release of HBpin is highly favoured while the product is still binding to the molecular recognition pocket.

(5) Although the X-ray data from the [ZnTPP ⊂ DMF] system (Fig. 2) displays a metal coordination of the carbonyl group *via* an sp^2-hybridized oxygen atom (Scheme 3, left), similar to that reported elsewhere for the binding of small DMF to zinc-porphyrin derivatives,[20g–o] the DFT-computed intermediates and transition states feature a slightly different type of coordination for the Zn···O=C interaction (Scheme 2). Here, the bulky tertiary benzamide is present in a zwitterionic form with a formal sp^3-hybridized oxygen atom engaged in coordination (Scheme 3, right), similarly to that observed by PM3 semi-empirical calculations (Fig. 2) and analogous to what has been reported elsewhere with zinc-porphyrins bound to bulky amides having the formula RCONMe$_2$ (R = alkyl, benzyl).[20a–f] Details concerning key bond distances and angles are displayed in Table S4 (see the ESI†). As such, the molecular recognition pocket is flexible enough to adopt different coordination geometries concerning the Zn···O=C interaction,[27] which becomes advantageous for this supramolecular catalysis.

(6) Supramolecular π–π interactions between the bounded benzamide substrate and the peripheral triazolylpyridine ligand are present according to non-covalent interaction NCI plots (Table S2 in the ESI†).

In order to experimentally validate the DFT-computed mechanism, which predicts that the C–H activation step is unexpectedly not rate-determining, kinetic isotope effect (KIE) experiments were carried out.[28] In order to have reliable data in a relatively short period of time, the reactions were carried out at 100 °C, which afforded good-quality fitting in the first 10 hours of the reaction. From two parallel experiments, one involving the benzamide starting material **1a** and the other one the deuterated **1a**-d_5, it was found that these reactions do follow a very similar kinetic profile (Fig. 5, top) within the error of the measurements (see the ESI†), thereby indicating an almost negligible kinetic isotope effect. Additionally, from intermolecular competition experiments between **1a** and **1a**-d_5, a very low KIE of 1.6 was observed (Fig. 5, bottom).

These experiments clearly indicate that the C–H activation event (**A** → **B**, Scheme 2) is not the rate-determining step for the supramolecular *ortho* C–H borylation of benzamides, which is unprecedented for remote iridium-catalysed C–H borylations so far, although it is known for cobalt-catalysed ones involving rationally designed pincer-type ligands.[17] As such, in our supramolecular iridium catalysis there is a formal change in the rate-determining step from pyridines[18] to benzamides. Whereas in pyridines the *meta*-C–H oxidative addition step is turnover limiting,[18] the C–B bond-forming step is the rate-determining one for the *ortho*-C–H borylation of benzamides. Overall, this is a unique case in which a different type of remote weak interaction (Zn···O=C *versus* Zn···N) in the secondary coordination sphere fundamentally changes the turnover limiting step in a catalytic cycle without altering the overall steric and electronic nature of the catalyst structure. It is relevant to note that ligand-free, directing-group-controlled iridium-catalysed C–H borylations can lead to low KIE with the C–H oxidative addition at iridium still being the rate-determining step,[29] which strikingly contrasts with the observations encountered in our supramolecular catalysis.[30]

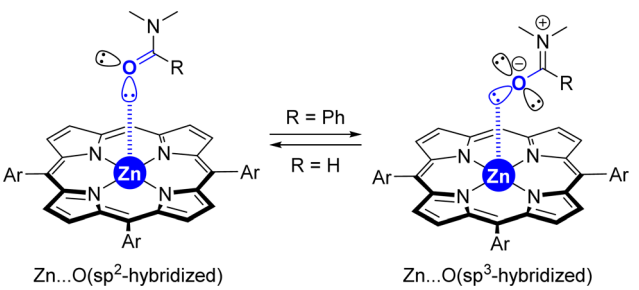

Scheme 3 Extreme cases in the difference of the coordination of small amides *versus* large amides to tetra-aryl-functionalized zinc-porphyrins.

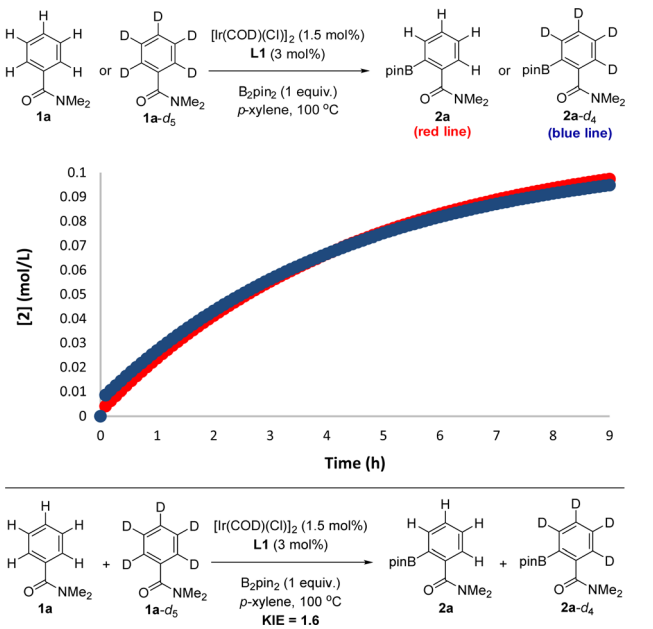

Fig. 5 Kinetic isotope effect (KIE) experiments relevant for mechanistic considerations: from two parallel reactions (top) and from an intermolecular competition (bottom).

Inhibition of side-product formation translates to superior catalysis: scope, limitations and overall reaction mechanism

Considering that high temperatures may facilitate overcoming the high reaction barrier (36.3 kcal mol^{-1}) found by DFT calculations (*vide supra*), we applied a temperature of 100 °C to the C–H borylation of benzamides using the most active and selective supramolecular ligand, namely **L1** (Table 1). After 24 hours, although the conversion of the starting material **1a** was higher at 100 °C than at 80 °C (90% *vs.* 83%) and the *ortho*-borylation reached a superior +99% selectivity (Table 1, entry 1), we observed formation of *ca.* 20% of deoxygenated borylated product **5** (Table 1, entry 1). We reasoned that the side-product **5** likely resulted from an iridium-catalysed deoxygenative reduction of amides *via* a hydroboration process with pinacolborane (HBpin) that forms at each turnover during the main iridium-catalysed borylation cycle.[31] To overcome this issue, we speculated that the cyclohexene additive could trap the *in situ* formed HBpin.[32] As such, not only could the side-product **5** be reduced but also the reactivity of the supramolecular catalyst could be increased by accelerating the HBpin release event that precedes catalyst regeneration according to the above-described DFT calculations.[33] In fact, the iridium-catalysed C–H bond borylation of benzamide **1a** performed in the presence of one equivalent of cyclohexene led to a comparable 94% conversion (Table 1, entry 2) as was observed in the absence of cyclohexene (90%, Table 1, entry 1) with an exclusive *ortho*-selectivity for both cases. Most notably, the side-product borylated amine **5** was reduced from 22% (Table 1, entry 1) to only trace amounts (Table 1, entry 2) when the reaction was carried out in the presence of the cyclohexene additive and the yield of mono-*ortho*-borylated benzamide **2a** increased from 60% (Table 1, entry 1) to 85% (Table 1, entry 2). Leaving the catalysis for longer time durations (30 hours) in the presence of cyclohexene led to full conversion of the starting material and complete *ortho*-selectivity in an 87% isolated yield of the *ortho*-mono-borylated benzamide **2a** (Table 1, entry 3).

With the optimal conditions in hand using the supramolecular ligand **L1** and cyclohexene as additive over 30 hours (Table 1, entry 3), we evaluated the substrate scope for this iridium-catalysed *ortho*-C–H borylation of tertiary benzamides directed by Zn···O=C weak interactions between the substrate and the catalyst (Table 2). Different steric patterns at the amide site (methyl, ethyl, iso-propyl) were tolerated including the case in which the amide is part of a piperidine fragment. The corresponding *ortho*-borylated products **2a–2d** were isolated in the range of 82–91% yields with full conversion of the

Table 1 Cyclohexene as an additive to suppress the formation of side-product **5** at 100 °C by further investigating the optimal reaction conditions[a]

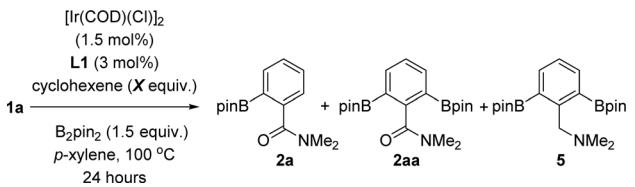

Entry	*X*	Conv. **1a** [b]	Yield **2a** [b]	Yield **2aa** [b]	Yield **5** [b]
1	0	90%	60%	8%	22%
2	1	94%	85%	4%	5%
3[c]	1	99%	91% (87%)[d]	4%	5%

[a] Reaction conditions: **1a** (0.024 g, 0.162 mmol), $[Ir(COD)(Cl)]_2$ (1.7 mg, 2.43×10^{-3} mmol), **L1** (4.1 mg, 4.86×10^{-3} mmol), B_2pin_2 (61.7 mg, 0.243 mmol), cyclohexene (13 mg, 16 μL, 0.162 mmol), *p*-xylene (1 mL), 100 °C, 24 hours. [b] Conversion of **1** and product selectivity were determined by GC analysis using dodecane as internal standard and ^1H NMR analysis. [c] Reaction performed over 30 hours. [d] Isolated yield displayed in brackets after purification by column chromatography.

Table 2 Scope evaluation of the iridium-catalysed supra-molecular *ortho*-selective C–H borylation of tertiary benzamides[a]

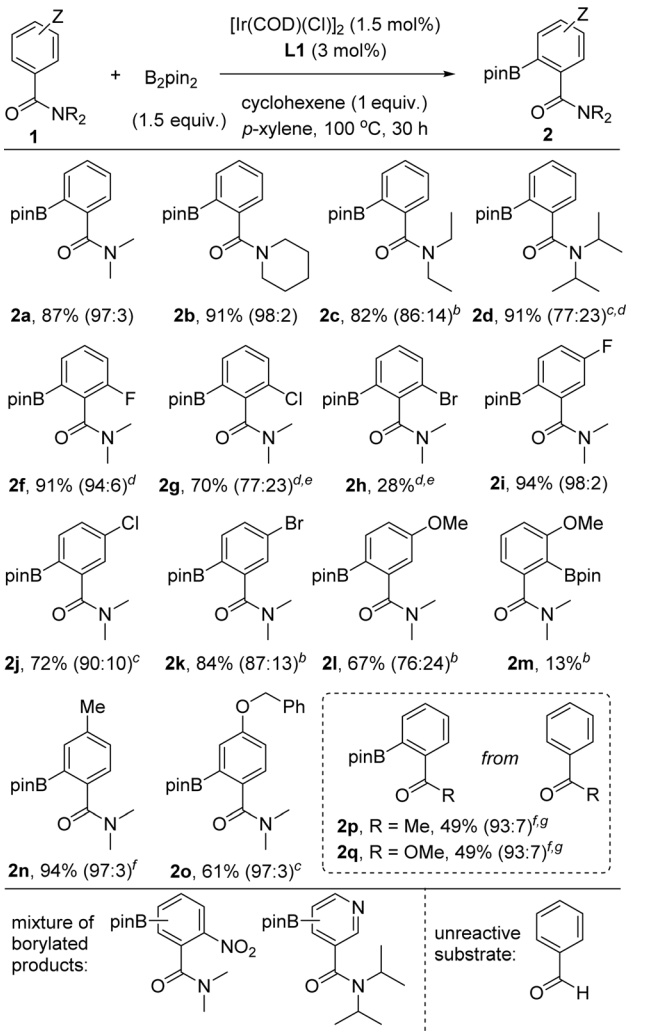

[a] Reaction conditions: **1** (0.162 mmol), $[Ir(COD)(Cl)]_2$ (1.7 mg, 2.43×10^{-3} mmol), **L1** (4.1 mg, 4.86×10^{-3} mmol), B_2pin_2 (61.7 mg, 0.243 mmol), cyclohexene (13 mg, 16 μL, 0.162 mmol), *p*-xylene (1 mL), 100 °C, 30 h (isolated yields after purification by column chromatography are reported and values in brackets correspond to the ratio between the *ortho*-regioisomer and other borylated products). [b] 40 hours. [c] 48 hours. [d] Without cyclohexene additive. [e] 72 hours. [f] 24 hours. [g] 80 °C.

corresponding starting materials **1a–1d** and an excellent *ortho*-selectivity (90–98%). These findings indicate also the benefits of performing the catalysis at higher temperatures for maximizing the dynamic coordination chemistry between the substrate and the catalyst *via* remote Zn···O=C weak interaction, as similarly observed for pyridine derivatives.[18c] As such, substrates that had room for improvement regarding their reactivity at 80 °C (**1b–1d**, Fig. 4) are efficiently borylated in the *ortho* position at 100 °C.

The catalysis tolerates halides such as fluoride, chloride and bromide in both *ortho* and *meta* positions in the aromatic ring as well as alkyl, benzyl and aryl substituents. The reactions appeared sensitive for the case in which the halide substituents are in the other *ortho* position. For instance, the *ortho*-borylated product **2f** containing a fluoride atom in the other *ortho* position was obtained in a remarkable 91% isolated yield whereas the yield gradually decreased from chloride (70% for **2g**) to bromide (28% for **2h**). We reasoned steric shielding between large substituents in the *ortho* position of the benzamide substrate and the porphyrin macrocycle and/or the *meso* phenyl substituents being at play regarding the structures of the DFT-computed intermediates and transition states (*vide supra*). Clearly, the reactivity for halide substituents follows a purely steric effect and not an electronic one, indirectly pointing out that the reactivity occurs when the substrate binds to the molecular recognition site of the supramolecular catalyst *via* remote Zn···O=C weak interaction. In the same vein, the *ortho*-borylated benzamides comprising less sterically demanding *meta*-functionalized fluoride (**2i**), chloride (**2j**) and bromide (**2k**) were isolated in 94%, 72% and 84% yields, respectively. In these cases, no C–H borylation took place in the *ortho* C–H bond between the amide and the halide groups. In contrast, a methoxy group placed in the *meta* position of the benzamide ring led to, besides the expected major borylated compound **2l** in 67% yield, 13% of **2m** in which the borylation occurred also at the *ortho*-C–H bond located between the amide and the methoxy group, thus indicating some directing group character for the methoxy group.[34] Tertiary benzamides comprising electronically different methyl and ether groups in the *para* position were compatible for the iridium-catalysed C–H bond *ortho*-borylation affording the corresponding products **2n** and **2o** in 94% and 61% isolated yields, respectively. In the case of benzamide **1o**, which comprises two aromatic groups, only the benzamide ring was prone to react by affording **2o**. A mixture of unidentified, borylated products was obtained when the substrate contained a nitro functional group (Table 2, bottom).

As could be expected considering our previous contributions,[18] using a pyridine derivative containing a tertiary amide group in the *meta* position afforded a mixture of borylated products as the nitrogen atom from pyridine and the carbonyl group from the amide are both engaged in binding to the zinc-porphyrin molecular recognition site. Next, we aimed at exploring other carbonyl-containing substrates different than amides **1** in the supramolecular iridium-catalysed *ortho*-C–H borylation (Table 2, framed). Acetophenone and methylbenzoate afforded the corresponding *ortho*-borylated products **2p** and **2q**, respectively, in promising 49% isolated yield in both cases. This observation also indirectly indicates the key role of the remote, weak Zn···O=C interaction in increasing the reactivity of the iridium catalyst. No reactivity was observed when using the very challenging benzaldehyde as the substrate.[35] It is relevant to note that the formation of deoxygenated side-products such as amine **5** (Table 1) was substrate-dependent, being not necessarily the use of the cyclohexene additive in several cases. As such, addition of cyclohexene might be regarded as a new tool for obtaining selective C–H borylations in challenging substrates.

Considering the many specificities presented by this supramolecular iridium catalysis as well as previous iridium-catalysed C–H bond borylations,[7–18] a reaction mechanism is proposed in Scheme 4. Initially, **Ir-1** species, which is a tris-boryl-iridium(COD) (COD = 1,5-cyclooctadiene) species coordinated to the triazolylpyridine site of **L1**, formed and further reacted with the benzamide substrate **1** liberating the COD ligand to afford intermediate **A**, in which the carbonyl group from the tertiary benzamide binds to the zinc centre of the porphyrin molecular recognition site. After selective *ortho*-C–H activation (**B**) and C–B bond formation at iridium (**C**), which is rate-determining (*vide supra*), the catalyst was regenerated with B_2pin_2 delivering one equivalent of HBpin. This catalyst regeneration may take place with the product still bound to the molecular recognition site as it could stabilize the transition

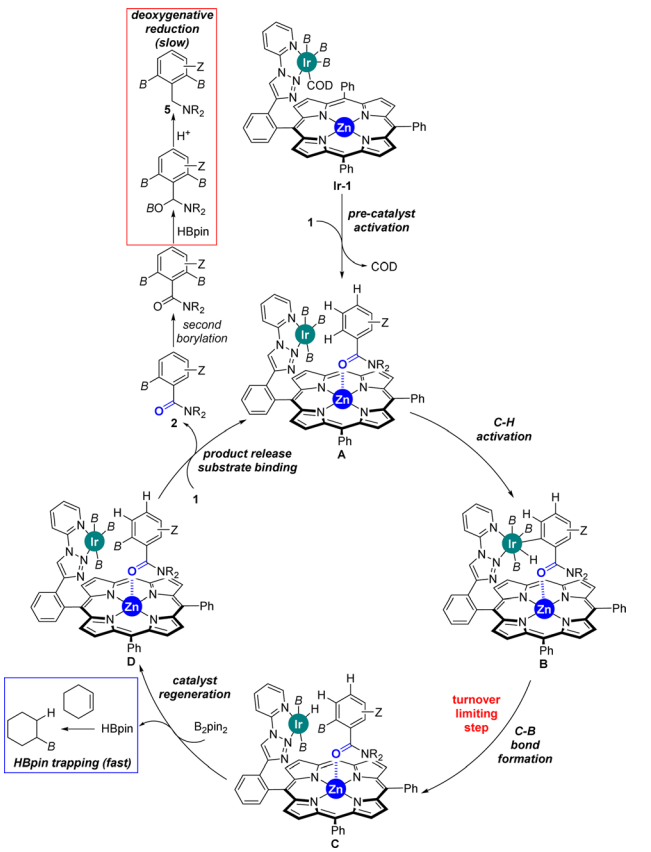

Scheme 4 Postulated reaction mechanism for the supramolecular iridium-catalysed *ortho*-selective C–H borylation of tertiary benzamides **1** using **L1**. *B* = (pinacolato)boron.

state *via* additional Ir···π interactions,[18b] as supported by DFT calculations (*vide supra*). Final product release and substrate binding enables the catalytic cycle (**D** → **A**) to be pursued. The generated HBpin at each turnover in the catalyst regeneration step **C** → **D** may partially serve to deoxygenate product **2** forming **5** (red frame, Scheme 4). However, the presence of stoichiometric amounts of cyclohexene in the reaction mixture suppresses this reaction pathway since the HBpin trapping event (blue frame, Scheme 4) is faster than the deoxygenative reduction (red frame, Scheme 4).

Conclusions

In summary, we have reported the use of Zn···O=C weak interactions to exert control on the reactivity of metal catalysts. In particular, we have demonstrated that the iridium-catalysed C–H bond borylations of tertiary benzamides occur in the *ortho* position when using a triazolylpyridine ligand equipped with a zinc-porphyrin molecular recognition site. The selectivity is exclusively dominated by the first coordination sphere of the catalyst since fine-tuning the triazolylpyridine fragment results in negligible changes regarding the regioselectivity ratio of the borylated products. Interestingly, the activity was controlled by the presence of the zinc-porphyrin backbone that brings the substrate close to the active site as demonstrated by a number of control experiments. Such behaviour is reminiscent of the Michaelis complex formed between a substrate and an enzyme in biological catalysis.[36] The optimization of the reaction conditions enabled the identification of $[Ir(COD)(Cl)]_2$ as a suitable precursor, which is rare for iridium-catalysed C–H borylations as most of the studies employed the more air sensitive $[Ir(COD)(OMe)]_2$.[18,37] Careful analysis of reaction conditions by mass balance analysis revealed the unexpected formation, in some cases, of a deoxygenated borylated side-product (**5**) resulting from the reaction of the HBpin formed during the catalyst regeneration with the borylated benzamide product **2**. This issue was circumvented by utilizing one equivalent of cyclohexene during the catalysis as a HBpin scavenger. In this way, *ortho*-borylated tertiary benzamides with a wide variety of functional groups at different positions were obtained according to a substrate evaluation. Preliminary studies indicate that enlarging the substrate scope to other oxygen-containing substrates is feasible. Importantly, detailed kinetic studies and DFT calculations shed light on the reaction mechanism showing that the C–H activation step is not the turnover limiting one in the catalytic cycle, which may explain the similar selectivity obtained for all supramolecular ligands (**L1–L6**). Overall, this contribution represents a unique case in which (i) not the selectivity but the activity is controlled by weak interactions at the secondary coordination sphere in transition metal-catalysed C–H functionalizations, (ii) a formal change in the rate-determining step for unbiased substrates is evidenced compared to state-of-the-art catalysts thanks to a supramolecular catalyst equipped with a well-defined substrate-recognition site, and (iii) a catalytic system previously known for *meta*-borylation switches its selectivity towards the *ortho*-regioisomer.

Data availability

The data supporting the findings of this study are available within the article and its ESI.†

Author contributions

JT: conceptualization, data curation, formal analysis, investigation, methodology, visualization, writing – original draft. VD: data curation, formal analysis, investigation, validation. MT: data curation, formal analysis, investigation, methodology, visualization. PR: data curation, formal analysis, investigation, validation. TR: data curation, formal analysis, investigation. AP: data curation, formal analysis, investigation, funding acquisition, methodology, project administration, supervision, validation, visualization. RGD: conceptualization, data curation, funding acquisition, methodology, project administration, supervision, visualization, writing – original draft, review & editing.

Conflicts of interest

There are no conflicts to declare.

Acknowledgements

The CNRS, University of Rennes, Fondation Rennes (MSc grant to P. R.), Agence Nationale de la Recherche (ANR-19-CE07-0039, PhD grant to J. T.) and Ministère de l'Enseignement supérieur et de la Recherche (PhD grant to V. D.) are acknowledged for financial support. A. P. is a Serra Húnter Fellow and recipient of ICREA Academia Prize 2019. A. P. thanks the Spanish Ministerio de Ciencia e Innovación for project PID2021-127423NB-I00 and the Generalitat de Catalunya for project 2021SGR623.

Notes and references

1 (*a*) M. C. White, *Science*, 2012, **335**, 807; (*b*) T. Gensch, M. N. Hopkinson, F. Glorius and J. Wencel-Delord, *Chem. Soc. Rev.*, 2016, **45**, 2900; (*c*) S. K. Sinha, S. Guin, S. Maiti, J. P. Biswas, S. Porey and D. Maiti, *Chem. Rev.*, 2022, **122**, 5682; (*d*) T. Dalton, T. Faber and F. Glorius, *ACS Cent. Sci.*, 2021, **7**, 245; (*e*) J. A. Labinger, *Chem. Rev.*, 2017, **117**, 8483; (*f*) K. Godula and D. Sames, *Science*, 2006, **312**, 67; (*g*) M. M. Diaz-Requejo and P. J. Perez, *Chem. Rev.*, 2008, **108**, 3379.

2 (*a*) T. Cernak, K. D. Dykstra, S. Tyagarajan, P. Vachal and S. W. Krska, *Chem. Soc. Rev.*, 2016, **45**, 546; (*b*) P. S. Fier and J. F. Hartwig, *Science*, 2013, **342**, 956; (*c*) W. Liu and J. T. Groves, *Acc. Chem. Res.*, 2015, **48**, 1727; (*d*) M. Simonetti, D. M. Cannas, X. Just-Baringo, I. J. Vitorica-Yrezabal and I. Larrosa, *Nat. Chem.*, 2018, **10**, 724; (*e*) J. Wencel-Delord and F. Glorius, *Nat. Chem.*, 2013, **5**, 369; (*f*) Y. Yang, J. Lan and J. You, *Chem. Rev.*, 2017, **117**, 8787; (*g*) J. F. Hartwig, *J. Am. Chem. Soc.*, 2016, **138**, 2; (*h*) Z. Dong, Z. Ren, S. J. Thompson, Y. Xu and G. Dong, *Chem. Rev.*, 2017, **117**, 9333.

3 (*a*) D. C. Blakemore, L. Castro, I. Churcher, D. C. Rees, A. W. Thomas, D. M. Wilson and A. Wood, *Nat. Chem.*, 2018, **10**, 383; (*b*) J. Yamaguchi, A. D. Yamaguchi and K. Itami, *Angew. Chem., Int. Ed.*, 2012, **51**, 8960; (*c*) L. Guillemard, N. Kaplaneris, L. Ackermann and M. J. Johansson, *Nat. Rev. Chem*, 2021, **5**, 522; (*d*) R. Jana, H. M. Begam and E. Dinda, *Chem. Commun.*, 2021, **57**, 10842; (*e*) R. R. Karimov and J. F. Hartwig, *Angew. Chem., Int. Ed.*, 2018, **57**, 4234; (*f*) L. McMurray, F. O'Hara and M. J. Gaunt, *Chem. Soc. Rev.*, 2011, **40**, 1885.

4 (*a*) D. J. Schipper and K. Fagnou, *Chem. Mater.*, 2011, **23**, 1594; (*b*) H. Bohra and M. Wang, *J. Mater. Chem. A*, 2017, **5**, 11550; (*c*) L. G. Mercier and M. Leclerc, *Acc. Chem. Res.*, 2013, **46**, 1597; (*d*) L. Xing and C. K. Luscombe, *J. Mater. Chem. C*, 2021, **9**, 16391; (*e*) Y. Segawa, T. Maekawa and K. Itami, *Angew. Chem., Int. Ed.*, 2015, **54**, 66; (*f*) I. A. Stepek and K. Itami, *ACS Mater. Lett.*, 2020, **2**, 951.

5 (*a*) D. A. Colby, R. G. Bergman and J. A. Ellman, *Chem. Rev.*, 2010, **110**, 624; (*b*) G. Rouquet and N. Chatani, *Angew. Chem., Int. Ed.*, 2013, **52**, 11726; (*c*) T. W. Lyons and M. S. Sanford, *Chem. Rev.*, 2010, **110**, 1147; (*d*) K. M. Engle, T.-S. Mei, M. Wasa and J.-Q. Yu, *Acc. Chem. Res.*, 2012, **45**, 788; (*e*) C. Sambiagio, D. Schönbauer, R. Blieck, T. Dao-Huy, G. Pototschnig, P. Schaaf, T. Wiesinger, M. F. Zia, J. Wencel-Delord, T. Besset, B. U. W. Maes and M. Schnürch, *Chem. Soc. Rev.*, 2018, **47**, 6603; (*f*) S. De Sarkar, W. Liu, S. I. Kozhushkov and L. Ackermann, *Adv. Synth. Catal.*, 2014, **356**, 1461; (*g*) P. B. Arockiam, C. Bruneau and P. H. Dixneuf, *Chem. Rev.*, 2012, **112**, 5879; (*h*) L. Ackermann, *Chem. Rev.*, 2011, **111**, 1315; (*i*) G. Meng, N. Y. S. Lam, E. L. Lucas, T. G. Saint-Denis, P. Verma, N. Chekshin and J.-Q. Yu, *J. Am. Chem. Soc.*, 2020, **142**, 10571; (*j*) R. Shang, L. Ilies and E. Nakamura, *Chem. Rev.*, 2017, **117**, 9086; (*k*) S. Rej, Y. Ano and N. Chatani, *Chem. Rev.*, 2020, **120**, 1788; (*l*) R.-Y. Zhu, M. E. Farmer, Y.-Q. Chen and J.-Q. Yu, *Angew. Chem., Int. Ed.*, 2016, **55**, 10578; (*m*) N. Kuhl, M. N. Hopkinson, J. Wencel-Delord and F. Glorius, *Angew. Chem., Int. Ed.*, 2012, **51**, 10236; (*n*) R. Gramage-Doria, *Chem.–Eur. J.*, 2020, **26**, 9688; (*o*) N. Y. S. Lam, Z. Fan, K. Wu, H. S. Park, S. Y. Shim, D. A. Strassfeld and J.-Q. Yu, *J. Am. Chem. Soc.*, 2022, **144**, 2793.

6 (*a*) K. Liao, S. Negretti, D. G. Musaev, J. Bacsa and H. M. L. Davies, *Nature*, 2016, **533**, 230; (*b*) Z. Zhang, K. Tanaka and J.-Q. Yu, *Nature*, 2017, **543**, 538; (*c*) O. Daugulis, H.-Q. Do and D. Shabashov, *Acc. Chem. Res.*, 2009, **42**, 1074; (*d*) P. Wang, P. Verma, G. Xia, J. Shi, J. X. Qiao, S. Tao, P. T. W. Cheng, M. A. Poss, M. E. Farmer, K.-S. Yeung and J.-Q. Yu, *Nature*, 2017, **551**, 489; (*e*) N. Della Ca, M. Fontana, E. Motti and M. Catellani, *Acc. Chem. Res.*, 2016, **49**, 1389; (*f*) D. Lichosyt, Y. Zhang, K. Hurej and P. Dydio, *Nat. Catal.*, 2019, **2**, 114; (*g*) R. Gramage-Doria and C. Bruneau, *Coord. Chem. Rev.*, 2021, **428**, 21362; (*h*) J. F. Hartwig and M. A. Larsen, *ACS Cent. Sci.*, 2016, **2**, 281; (*i*) M. T. Mihai, G. R. Genova and R. J. Phipps, *Chem. Soc. Rev.*, 2018, **47**, 149.

7 (*a*) I. A. I. Mkhalid, J. H. Barnard, T. B. Marder, J. M. Murphy and J. F. Hartwig, *Chem. Rev.*, 2010, **110**, 890; (*b*) R. Bisht, C. Haldar, M. M. M. Hassan, M. E. Hoque, J. Chaturvedi and B. Chattopadhyay, *Chem. Soc. Rev.*, 2022, **51**, 5042; (*c*) L. Xu, G. Wang, S. Zhang, H. Wang, L. Wang, L. Liu, J. Jiao and P. Li, *Tetrahedron*, 2017, **73**, 7123; (*d*) J. S. Wright, P. J. H. Scott and P. G. Steel, *Angew. Chem., Int. Ed.*, 2021, **60**, 2796; (*e*) Y. Kuroda, K. Park, Y. Shimazaki, R.-L. Zhong, S. Sakaki and Y. Nakao, *Angew. Chem., Int. Ed.*, 2023, **62**, e202300704; (*f*) M. M. M. Hassan, S. Guria, S. Dey, J. Das and B. Chattopadhyay, *Sci. Adv.*, 2023, **9**, eadg3311; (*g*) M. R. Smith III, R. Bisht, C. Haldar, G. Pandey, J. E. Dannatt, B. Ghaffari, R. E. Maleczka Jr and B. Chattopadhyay, *ACS Catal.*, 2018, **8**, 6216; (*h*) S. Guria, M. M. M. Hassan and B. Chattopadhyay, *Org. Chem. Front.*, 2024, **11**, 929.

8 (*a*) D. G. Hall, *Boronic Acids. Preparation, Applications in Organic Synthesis*, Wiley-VCH, Weinheim, 2011; (*b*) E. C. Neeve, S. J. Geier, I. A. I. Mkhalid, S. A. Westcott and T. B. Marder, *Chem. Rev.*, 2016, **116**, 9091.

9 (*a*) J. Takagi, K. Sato, J. F. Hartwig, T. Ishiyama and N. Miyaura, *Tetrahedron Lett.*, 2002, **43**, 5649; (*b*) T. Ishiyama, Y. Nobuta, J. F. Hartwig and N. Miyaura, *Chem. Commun.*, 2003, 2924; (*c*) M. A. Larsen, R. J. Oeschger and J. F. Hartwig, *ACS Catal.*, 2020, **10**, 3415; (*d*) M. A. Larsen, C. V. Wilson and J. F. Hartwig, *J. Am. Chem. Soc.*, 2015, **137**, 8633; (*e*) R. Oeschger, B. Su, Y. Yu, C. Ehinger, E. Romero, S. He and J. Hartwig, *Science*, 2020, **368**, 736; (*f*) O. Kuleshova, S. Asako and L. Ilies, *ACS Catal.*, 2021, **11**, 5968; (*g*) C. Haldar, M. E. Hoque, J. Chaturvedi, M. M. M. Hassan and B. Chattopadhyay, *Chem. Commun.*, 2021, **57**, 13059; (*h*) M. E. Hoque, S. Dey, M. M. M. Hassan, J. Chaturvedi, S. Guria, J. Das, B. Roy and B. Chattopadhyay, *Tetrahedron Chem*, 2022, **3**, 100028.

10 (*a*) E. Fernandez, *Top. Organomet. Chem.*, 2020, **69**, 207; (*b*) T. Ishiyama, J. Takagi, K. Ishida, N. Miyaura, N. R. Anastasi and J. F. Hartwig, *J. Am. Chem. Soc.*, 2002, **124**, 390; (*c*) T. Ishiyama, J. Takagi, J. F. Hartwig and N. Miyaura, *Angew. Chem., Int. Ed.*, 2002, **41**, 3056; (*d*) C. W. Liskey, C. S. Wei, D. R. Pahlsa and J. F. Hartwig, *Chem. Commun.*, 2009, 5603; (*e*) R. J. Oeschger, M. A. Larsen, A. Bismuto and J. F. Hartwig, *J. Am. Chem. Soc.*, 2019, **141**, 16479; (*f*) A. Ros, R. Fernandez and J. M. Lassaletta, *Chem. Soc. Rev.*, 2014, **43**, 3229; (*g*) J. Chaturvedi, C. Haldar, R. Bisht, G. Pandey and B. Chattopadhyay, *J. Am. Chem. Soc.*, 2021, **143**, 7604; (*h*) C. Haldar, R. Bisht, J. Chaturvedi, S. Guria, M. M. M. Hassan, B. Ram and B. Chattopadhyay, *Org. Lett.*, 2022, **24**, 8147; (*i*) S. Guria, M. M. M. Hassan, J. Ma, S. Dey, Y. Liang and B. Chattopadhyay, *Nat. Commun.*, 2023, **14**, 6906.

11 (*a*) W. Chang, Y. Chen, S. Lu, H. Jiao, Y. Wang, T. Zheng, Z. Shi, Y. Han, Y. Lu, Y. Wang, Y. Pan, J.-Q. Yu, K. N. Houk, F. Liu and Y. Liang, *Chem*, 2022, **8**, 1775; (*b*) S. Pandit, S. Maiti and D. Maiti, *Org. Chem. Front.*, 2021, **8**, 4349; (*c*) X. Zou and S. Xu, *Chin. J. Org. Chem.*, 2021, **41**, 2610; (*d*) J. Wang, T. Torigoe and Y. Kuninobu, *Org. Lett.*,

2019, **21**, 1342; (*e*) X. Lu, Y. Yoshigoe, H. Ida, M. Nishi, M. Kanai and Y. Kuninobu, *ACS Catal.*, 2019, **9**, 1705; (*f*) H. J. Davis, M. T. Mihai and R. J. Phipps, *J. Am. Chem. Soc.*, 2016, **138**, 12759; (*g*) B. Lee, M. T. Mihai, V. Stojalnikova and R. J. Phipps, *J. Org. Chem.*, 2019, **84**, 13124; (*h*) M. T. Mihai, H. J. Davis, G. R. Genov and R. J. Phipps, *ACS Catal.*, 2018, **8**, 3764; (*i*) M. E. Hoque, R. Bisht, C. Haldar and B. Chattopadhyay, *J. Am. Chem. Soc.*, 2017, **139**, 7745; (*j*) Y. Wang, W. Chang, S. Qin, H. Ang, J. Ma, S. Lu and Y. Liang, *Angew. Chem., Int. Ed.*, 2022, **61**, e202206797; (*k*) J. L. Douthwaite and R. J. Phipps, *Tetrahedron*, 2022, **117–118**, 132831; (*l*) R. Bisht and B. Chattopadhyay, *J. Am. Chem. Soc.*, 2016, **138**, 84; (*m*) R. Bisht, J. Chaturvedi, G. Pandey and B. Chattopadhyay, *Org. Lett.*, 2019, **21**, 6476.

12 M. Ditzen, M. Pellegrino and L. B. Vosshall, *Science*, 2008, **319**, 1838.

13 (*a*) G. A. Bakken and P. C. Jurs, *J. Med. Chem.*, 2000, **43**, 4534; (*b*) X. He, A. Alianc and P. R. Ortiz de Montellano, *Bioorg. Med. Chem.*, 2007, **15**, 6649; (*c*) M. A. Letavic, L. Aluisio, R. Apodaca, M. Bajpai, A. J. Barbier, A. Bonneville, P. Bonaventure, N. I. Carruthers, C. Dugovic, I. C. Fraser, M. L. Kramer, B. Lord, T. W. Lovenberg, L. Y. Li, K. S. Ly, H. Mcallister, N. S. Mani, K. L. Morton, A. Ndifor, S. D. Nepomuceno, C. R. Pandit, S. B. Sands, C. R. Shah, J. E. Shelton, S. S. Snook, D. M. Swanson and W. Xiao, *ACS Med. Chem. Lett.*, 2015, **6**, 450; (*d*) C. J. Gerry and S. L. Schreiber, *Nat. Rev. Drug Discovery*, 2018, **17**, 333.

14 (*a*) L. Yang, K. Semba and Y. Nakao, *Angew. Chem., Int. Ed.*, 2017, **56**, 4853; (*b*) M. E. Hoque, R. Bisht, A. Unnikrishnan, S. Dey, M. M. M. Hassan, S. Guria, R. N. Rai, R. B. Sunoj and B. Chattopadhyay, *Angew. Chem., Int. Ed.*, 2022, **61**, e202203539; (*c*) R. Bisht, M. E. Hoque and B. Chattopadhyay, *Angew. Chem., Int. Ed.*, 2018, **57**, 15762; (*d*) Y. Kuninobu, H. Ida, M. Nishi and M. Kanai, *Nat. Chem.*, 2015, **7**, 712; (*e*) S. Lu, T. Zheng, J. Ma, Z. Deng, S. Qin, Y. Chen and Y. Liang, *Angew. Chem., Int. Ed.*, 2022, **61**, e202201285; (*f*) L. Yang, N. Uemura and Y. Nakao, *J. Am. Chem. Soc.*, 2019, **141**, 7972.

15 (*a*) S.-T. Bai, C. B. Bheeter and J. N. H. Reek, *Angew. Chem., Int. Ed.*, 2019, **58**, 13039; (*b*) C. Liu, L. Zhang, L. Li and M. Lei, *J. Org. Chem.*, 2021, **86**, 16858.

16 (*a*) J. E. Dannatt, A. Yadav, M. R. Smith III and R. E. Maleczka Jr, *Tetrahedron Lett.*, 2022, **109**, 132578; (*b*) B. Ghaffari, S. M. Preshlock, D. L. Plattner, R. J. Staples, P. E. Maligres, S. W. Krska, R. E. Maleczka Jr and M. R. Smith III, *J. Am. Chem. Soc.*, 2014, **136**, 14345; (*c*) M. E. Hoque, M. M. M. Hassan and B. Chattopadhyay, *J. Am. Chem. Soc.*, 2021, **143**, 5022; (*d*) G. Wang, L. Liu, H. Wang, Y.-S. Ding, J. Zhou, S. Mao and P. Li, *J. Am. Chem. Soc.*, 2017, **139**, 91; (*e*) J. Jiao, W. Nie, P. Song and P. Li, *Org. Biomol. Chem.*, 2021, **19**, 355; (*f*) D. Marcos-Atanes, C. Vidal, C. D. Navo, F. Peccati, G. Jiménez-Osés and J. L. Mascareñas, *Angew. Chem., Int. Ed.*, 2023, **62**, e202214510; (*g*) S. Kawamorita, H. Ohmiya, K. Hara, A. Fukuoka and M. Sawamura, *J. Am. Chem. Soc.*, 2009, **131**, 5058; (*h*) H. L. Li, Y. Kuninobu and M. Kanai, *Angew. Chem., Int. Ed.*, 2017, **56**, 1495; (*i*) H.-L. Li, M. Kanai and Y. Kuninobu, *Org. Lett.*, 2017, **19**, 5944; (*j*) J. Zeng, M. Naito, T. Torigoe, M. Yamanaka and Y. Kuninobu, *Org. Lett.*, 2020, **22**, 3485; (*k*) Y. Kuninobu, T. Iwanaga, T. Omura and K. Takai, *Angew. Chem., Int. Ed.*, 2013, **52**, 4431; (*l*) Y. Yoshigoe and Y. Kuninobu, *Org. Lett.*, 2017, **19**, 3450; (*m*) J. M. Zakis, A. M. Messinis, L. Ackermann, T. Smejkal and J. Wencel-Delord, *Adv. Synth. Catal.*, 2024, **366**, 2292.

17 (*a*) J. V. Obligacion, S. P. Semproni, I. Pappas and P. J. Chirik, *J. Am. Chem. Soc.*, 2016, **138**, 10645; (*b*) J. V. Obligacion and P. J. Chirik, *ACS Catal.*, 2017, **7**, 4366; (*c*) H. Li, J. V. Obligacion, P. J. Chirik and M. B. Hall, *ACS Catal.*, 2018, **8**, 10606; (*d*) T. P. Pabst, J. V. Obligacion, E. Rochette, I. Pappas and P. J. Chirik, *J. Am. Chem. Soc.*, 2019, **141**, 15378; (*e*) R. Arevalo, T. P. Pabst and P. J. Chirik, *Organometallics*, 2020, **39**, 2763; (*f*) T. P. Pabst, L. Quach, K. T. MacMillan and P. J. Chirik, *Chem*, 2021, **7**, 237.

18 (*a*) J. Trouvé, P. Zardi, S. Al-Shehimy, T. Roisnel and R. Gramage-Doria, *Angew. Chem., Int. Ed.*, 2021, **60**, 18006; (*b*) M. Tomasini, L. Caporaso, J. Trouvé, J. Poater, R. Gramage-Doria and A. Poater, *Chem.–Eur. J.*, 2022, **28**, e202201970; (*c*) J. Trouvé, P. Rajeshwaran, M. Tomasini, A. Perennes, T. Roisnel, A. Poater and R. Gramage-Doria, *ACS Catal.*, 2023, **13**, 7715.

19 Deposition Number 2216009 (ZnTPP ⊂ DMF) contains the supplementary crystallographic data for this paper. These data are provided free of charge by the Cambridge Crystallographic Data Centre†

20 (*a*) M. M. Williamson, C. M. Prosser-McCartha, S. Mukundan Jr and C. L. Hill, *Inorg. Chem.*, 1988, **27**, 1061; (*b*) S. Lipstman, S. Muniappan and I. Goldberg, *Acta Crystallogr., Sect. E: Struct. Rep. Online*, 2006, **62**, m2330; (*c*) B. Boitrel, V. Baveux-Chambenoît and P. Richard, *Eur. J. Org Chem.*, 2001, 4213; (*d*) L. H. Tong, P. Pengo, W. Clegg, J. P. Lowe, P. R. Raithby, J. K. M. Sanders and S. I. Pascu, *Dalton Trans.*, 2011, **40**, 10833; (*e*) L. Carlucci, G. Ciani, D. M. Proserpio and F. Porta, *CrystEngComm*, 2005, **7**, 78; (*f*) G. Huang, C.-K. Tsang, Z. Xu, K. Li, M. Zeller, A. D. Hunter, S. S.-Y. Chui and C.-M. Che, *Cryst. Growth Des.*, 2009, **9**, 1444; (*g*) S. J. Rodgers, C. A. Koch, J. R. Tate, C. A. Reed, C. W. Eigenbrot and W. R. Scheidt, *Inorg. Chem.*, 1987, **26**, 3647; (*h*) C. A. Swamy and P. Thilagar, *Chem.–Eur. J.*, 2015, **21**, 8874; (*i*) Y. Zhu, Y. Huang, Q. Li, D. Zang, J. Gu, Y. Tang and Y. Wei, *Inorg. Chem.*, 2020, **59**, 2575; (*j*) R. Rubbiani, W. Wu, A. Naik, M. Larocca, L. Schneider, R. Padrutt, V. Babu, C. Konig, D. Hinger, C. Maake, S. Ferrari, G. Gasser and B. Spingler, *Chem. Commun.*, 2020, **56**, 14373; (*k*) I. Goldberg and A. Karmakar, *CrystEngComm*, 2010, **12**, 4095; (*l*) T. Nakamura, H. Ube, M. Shiro and M. Shionoya, *Angew. Chem., Int. Ed.*, 2013, **52**, 720; (*m*) E. Nichols, J. S. Derrick, S. K. Nistanaki, P. T. Smith and C. J. Chang, *Chem. Sci.*, 2018, **9**, 2952; (*n*) H. Huang, H. Sato, J. Pirillo, Y. Hijikata, Y. S. Zhao, S. Z. D. Cheng and T. Aida, *J. Am. Chem. Soc.*, 2021, **143**, 15319; (*o*) D. K. Kumar, A. Das and P. Dastidar, *Inorg. Chem.*, 2007, **46**, 7351.

21 (*a*) R. G. Pearson, *J. Am. Chem. Soc.*, 1963, **85**, 3533; (*b*) R. G. Parr and R. G. Pearson, *J. Am. Chem. Soc.*, 1983, **105**, 7512; (*c*) R. G. Pearson, *Coord. Chem. Rev.*, 1990, **100**, 403.

22 J.-Y. Cho, C. N. Iverson and M. R. Smith, *J. Am. Chem. Soc.*, 2000, **122**, 12868.

23 (*a*) M. Kadri, J. Hou, V. Dorcet, T. Roisnel, L. Bechki, A. Miloudi, C. Bruneau and R. Gramage-Doria, *Chem.–Eur. J.*, 2017, **23**, 5033; (*b*) P. Zardi, T. Roisnel and R. Gramage-Doria, *Chem.–Eur. J.*, 2019, **25**, 627; (*c*) N. Abuhafez and R. Gramage-Doria, *Faraday Discuss.*, 2023, **244**, 186.

24 (*a*) K. M. Kadish, K. M. Smith and R. Guilard, *Handbook of Porphyrin Science*, World Scientific, Singapore, vol. 1–44, 2010; (*b*) I. Beletskaya, V. S. Tyurin, A. Y. Tsivadze, R. Guilard and C. Stern, *Chem. Rev.*, 2009, **109**, 1659.

25 (*a*) R. P. Bonar-Law, L. G. Mackay, C. J. Walter, V. Marvaud and J. K. M. Sanders, *Pure Appl. Chem.*, 1994, **66**, 803; (*b*) J. K. M. Sanders, *Pure Appl. Chem.*, 2000, **72**, 2265.

26 D. W. Robbins and J. F. Hartwig, *Angew. Chem., Int. Ed.*, 2013, **52**, 933.

27 (*a*) H. Sigel and R. B. Martin, *Chem. Rev.*, 1982, **82**, 385; (*b*) S. Adachi, N. Kumagai and M. Shibasaki, *Chem. Sci.*, 2017, **8**, 85; (*c*) The calculated MBO values in the solvent phase of the Zn···O=C interaction are 0.138 for benzamide substrate and 0.122 of the Zn···N interaction for pyridine substrate.

28 (*a*) W. D. Jones, *Acc. Chem. Res.*, 2003, **36**, 140; (*b*) S. A. Blum, K. L. Tan and R. G. Bergman, *J. Org. Chem.*, 2003, **68**, 4127; (*c*) G. Parkin, *Acc. Chem. Res.*, 2009, **42**, 315; (*d*) M. Gómez-Gallego and M. A. Sierra, *Chem. Rev.*, 2011, **111**, 4857; (*e*) E. M. Simmons and J. F. Hartwig, *Angew. Chem., Int. Ed.*, 2012, **51**, 3066; (*f*) Z. Mao and C. T. Campbell, *ACS Catal.*, 2020, **10**, 4181; (*g*) X. Gao, X.-Y. Yua and C.-R. Chang, *Phys. Chem. Chem. Phys.*, 2022, **24**, 15182.

29 M. M. M. Hassan, B. Mondal, S. Singh, C. Haldar, J. Chaturvedi, R. Bisht, R. B. Sunoj and B. Chattopadhyay, *J. Org. Chem.*, 2022, **87**, 4360.

30 A low KIE effect has recently been reported for directing-group-controlled iridium-catalyzed C–H borylation in which the rate-determining step is the isomerization of the iridium(III) C–H-activated complex, see: N. Le, N. L. Chuang, C. M. Oliver, A. V. Samoshin, J. T. Hemphill, K. C. Morris, S. N. Hyland, H. Gua, Ch. E. Webster and T. B. Clark, *ACS Catal.*, 2023, **13**, 12877.

31 (*a*) C. J. Barger, R. D. Dicken, V. L. Weidner, A. Motta, T. L. Lohr and T. J. Marks, *J. Am. Chem. Soc.*, 2020, **142**, 8019; (*b*) M. K. Bisai, K. Gour, T. Das, K. Vanka and S. S. Sen, *Dalton Trans.*, 2021, **50**, 2354; (*c*) P. Ghosh and J. A. von Wangelin, *Angew. Chem., Int. Ed.*, 2021, **60**, 16035; (*d*) M.-L. Yuan, J.-H. Xie, S.-F. Zhu and Q.-L. Zhou, *ACS Catal.*, 2016, **6**, 3665.

32 (*a*) D. J. Pasto and J. Hickman, *J. Am. Chem. Soc.*, 1968, **90**, 4445; (*b*) D. J. Pasto, J. Chow and S. K. Arora, *Tetrahedron*, 1969, **25**, 1557; (*c*) J. Niziol and T. Ruman, *Lett. Org. Chem.*, 2012, **9**, 257; (*d*) Y. Yamamoto, R. Fujikawa, T. Umemoto and N. Miyaura, *Tetrahedron*, 2004, **60**, 10695; (*e*) L. P. Press, A. J. Kosanovich, B. J. McCulloch and O. V. Ozerov, *J. Am. Chem. Soc.*, 2016, **138**, 9487.

33 H. Tamura, H. Yamazaki, H. Sato and S. Sakaki, *J. Am. Chem. Soc.*, 2003, **125**, 16114.

34 (*a*) B. A. Vanchura II, S. M. Preshlock, P. C. Roosen, V. A. Kallepalli, R. J. Staples, R. E. Maleczka Jr, D. A. Singleton and M. R. Smith III, *Chem. Commun.*, 2010, **46**, 7724; (*b*) K. Yamazaki, S. Kawamorita, H. Ohmiya and M. Sawamura, *Org. Lett.*, 2010, **12**, 3978; (*c*) B. Chattopadhyay, J. E. Dannatt, I. L. Andujar-De Sanctis, K. A. Gore, R. E. Maleczka Jr, D. A. Singleton and M. R. Smith III, *J. Am. Chem. Soc.*, 2017, **139**, 7864.

35 Replacing the amide group in the substrate **1** by a sulfone, namely methyphenylsulfone, provided a mono-borylated product in a very modest 27% yield, being not possible to isolate it for further characterization unfortunately.

36 (*a*) V. L. Schramm, *Acc. Chem. Res.*, 2015, **48**, 1032; (*b*) B. Ma, S. Kumar, C. J. Tsai, Z. Hu and R. Nussinov, *J. Theor. Biol.*, 2000, **203**, 383; (*c*) Y. Peng, A. L. Hansen, L. Bruschweiler-Li, O. Davulcu, J. J. Skalicky, M. S. Chapman and R. Brüschweiler, *J. Am. Chem. Soc.*, 2017, **139**, 4846.

37 (*a*) C. C. C. Johansson Seechurn, V. Sivakumar, D. Satoskar and T. J. Colacot, *Organometallics*, 2014, **33**, 3514; (*b*) E. D. Slack and T. J. Colac ot, *Org. Lett.*, 2021, **23**, 1561.